NUCL SCI TECH (2018) 29:110
https://doi.org/10.1007/s41365-018-0458-1

Effects of fuel salt composition on fuel salt temperature coefficient (FSTC) for an under-moderated molten salt reactor (MSR)

Xiao-Xiao Li[1,2] · Yu-Wen Ma[1,2,3] · Cheng-Gang Yu[1,2] · Chun-Yan Zou[1,2,3] · Xiang-Zhou Cai[1,2,3] · Jin-Gen Chen[1,2,3]

Received: 7 February 2018 / Revised: 27 April 2018 / Accepted: 2 May 2018 / Published online: 3 July 2018

Abstract With respect to a liquid-fueled molten salt reactor (MSR), the temperature coefficient of reactivity mainly includes the moderator temperature coefficient (MTC) and the fuel salt temperature coefficient (FSTC). The FSTC is typically divided into the Doppler coefficient and the density coefficient. In order to compensate for the potentially positive MTC, the FSTC should be sufficiently negative, and this is mostly optimized in terms of the geometry aspect in pioneering studies. However, the properties of fuel salt also directly influence the FSTC. Thus, the effects of different fuel salt compositions including the ^{235}U enrichment, heavy metal proportion in salt phase (HM proportion), and the ^{7}Li enrichment on FSTC are investigated from the viewpoint of the essential six-factor formula. The analysis is based on an under-moderated MSR. With respect to the Doppler coefficient, the temperature coefficient of the fast fission factors ($\alpha_T(\varepsilon)$) is positive and those of the resonance escape probability ($\alpha_T(p)$), thermal reproduction factor ($\alpha_T(\eta)$), thermal utilization factor ($\alpha_T(f)$), and total non-leakage probability ($\alpha_T(\Lambda)$) are negative. With respect to the density coefficient, $\alpha_T(p)$ and $\alpha_T(\eta)$ are positive, while the others are negative. The results indicate that the effects of the ^{235}U enrichment and HM on FSTC are mainly reflected in $\alpha_T(\varepsilon)$ and $\alpha_T(p)$, which are the dominant factors when the neutron spectrum is relatively hard. Furthermore, the ^{7}Li enrichment influences FSTC by $\alpha_T(f)$ and $\alpha_T(\Lambda)$, which are the key factors in a relative soft spectrum. In order to obtain a more negative FSTC for an under-moderated MSR, the possible positive density coefficient, especially its $\alpha_T(p)$, should be suppressed. Thus, a lower ^{235}U enrichment (albeit higher than a certain value, 5 wt% in this article) along with a lower HM proportion and/or a higher ^{7}Li enrichment are recommended. The analyses provide an approach to achieve a more suitable fuel salt composition with a sufficiently negative FSTC.

Keywords Molten salt reactor (MSR) · Fuel salt temperature coefficient (FSTC) · Six-factor formula

This work was supported by the Chinese TMSR Strategic Pioneer Science and Technology Project (No. XDA02010000) and the Frontier Science Key Program of the Chinese Academy of Sciences (No. QYZDY-SSW-JSC016).

✉ Xiao-Xiao Li
lixiaoxiao@sinap.ac.cn

Xiang-Zhou Cai
caixz@sinap.ac.cn

Jin-Gen Chen
chenjg@sinap.ac.cn

1 Shanghai Institute of Applied Physics, Chinese Academy of Sciences, Shanghai 201800, China

2 CAS Innovative Academies in TMSR Energy System, Chinese Academy of Sciences, Shanghai 201800, China

3 University of Chinese Academy of Sciences, Beijing 100049, China

1 Introduction

The molten salt reactor (MSR) [1, 2], being one of the six types of nuclear fission reactors retained in the framework of the Generation IV International Forum (GIF) [3], has attracted increasing attention, and two categories have been developed of it. In the first category known as the liquid-fueled MSR (MSR-LF) [4, 5], nuclear fuel is dissolved in the molten salt to form a fuel salt mixture that acts both as coolant and fuel. In the second category, i.e., the solid-fueled MSR (MSR-SF), molten salt acts only as the primary coolant of a coated particle fueled reactor typically termed as a Fluoride salt-cooled high-temperature reactor (FHR) [6, 7]. When compared with FHR, MSR-LF possesses unique characteristics such as online or batched fuel processing that benefited from a liquid fuel salt and higher fuel economy due to the absence of fuel assembly preparation.

When compared with the traditional light water reactor (LWR), MSR can provide an extremely high outlet temperature based on the special characteristics of molten salt, especially, high boiling point and high volumetric heat capacity [8, 9]. Thus, the reactor core temperature alters significantly between the normal operation (hot) state and the shutdown (cold) state and subsequently leads to a large variation in reactivity by means of several factors including the Doppler broadening and neutron spectrum shifting. Furthermore, the magnitude of the reactivity change directly influences the reactivity control system. Therefore, the temperature coefficient is a crucial factor for reactor safety.

With respect to a graphite-moderated MSR with liquid fuel, the temperature coefficient is primarily determined by the moderator temperature coefficient (MTC) and fuel salt temperature coefficient (FSTC) [10]. An increase in the moderator temperature causes a shift in the Maxwellian spectrum to higher neutron energies [11] and results in a higher fast fission factor, i.e., a positive contribution to MTC. Furthermore, competition between the microscopic capture cross section of the fertile materials (for e.g., ^{238}U, ^{232}Th, etc.) and the microscopic fission cross section of the fissile nuclides (for e.g., ^{233}U, ^{235}U, and ^{239}Pu) makes the MTC either negative or positive based on the neutron spectrum and the fissile-to-fertile ratio [12]. Over the past few years, issues concerning positive MTC were reported or discussed for several designs of graphite-moderated MSRs such as molten salt breeder reactor (MSBR) [11, 13, 14] and thorium molten salt reactor (TMSR) [11, 15]. The positive MTC may lead to severe transient behaviors, according to the transient analysis [14]. Moreover, the fuel loading, operation temperature, and burn-up also influence the MTC.

In order to compensate for the possible positive contribution of MTC, a sufficiently negative FSTC is required in the design of an MSR from the aspect of reactor self-regulation. Typically, two divided separate effects are adopted (Doppler coefficient and density coefficient) [16, 17] to analyze their respective contribution to FSTC. The Doppler coefficient characterizes the broadening of the low-lying absorption resonances (the capture and/or fission) of the stronger absorbers (^{232}Th, ^{238}U, and ^{240}Pu) (http://www.nndc.bnl.gov/exfor/endf00.jsp). Increases in the fuel salt temperature cause a widening resonance and subsequently lead to a decrease in the resonance escape probability, and thus the Doppler coefficient is typically negative. The density coefficient is a combination of the graphite–salt volume ratio, absorption of heavy metal, and core leakage. When the fuel salt temperature increases, the fuel salt density tends to be smaller since a small fraction of salt is expelled from the reactor core, causing a decrease in the fuel concentration and the neutron spectrum to simultaneously become softer. It can result in an increase in absorption cross section of fuel nuclide. Furthermore, the above phenomena may result in an increase in the fast fission of fuel nuclide. Thus, the density coefficient might be either positive or negative. Based on the above concerns, the FSTC is a superimposed effect in the safe operation of a MSR and therefore should be carefully analyzed. Most studies on FSTC have focused on the geometry optimization [15, 18, 19], especially in the graphite–salt volume ratio for graphite assembly with different shapes.

Given the significant influences of fuel salt composition on FSTC for MSR-LF, it is extremely important to evaluate the effects of fuel salt composition on FSTC. Additionally, most pioneering studies employed the four-factor formula in the physical design of a reactor to understand the trends of the temperature coefficient without considering neutron leakage [20–22]. As mentioned above, the reduced fuel salt density can cause an increase in the neutron leakage from the core. Therefore, a six-factor formula is more suitable to understand FSTC on a core level as opposed to the four-factor formula on an assembly level. Thus, the six-factor formula is introduced to perform a quantitative analysis on FSTC.

This paper is organized as follows. Section 2 describes the reactor parameters and numerical simulation to calculate FSTC. Section 3 presents the theoretical explanation of FSTC via the six-factor formula and discusses the fuel salt composition effects on FSTC including the fissile enrichment, heavy metal proportion, and the ^{7}Li enrichment. Finally, conclusions are given in Sect. 4.

2 Analyses methodology

2.1 Simulation model specification

The reactor model of MSR used in the study has a simplified cylindrical geometry (Fig. 1) and is composed of an active zone and a surrounding reflector. The active zone was filled with graphite–salt lattices with a salt volume

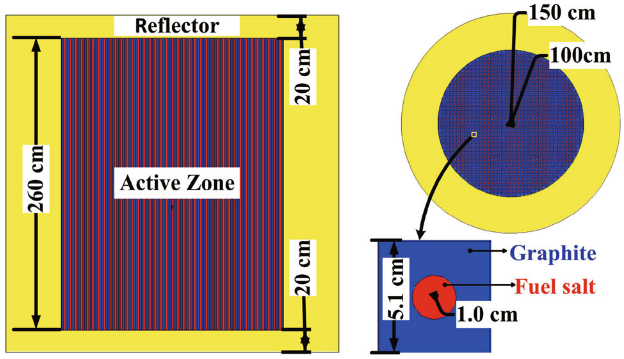

Fig. 1 (Color online) The schematic diagram of the reactor core of MSR

fraction (the volume of fuel salt over that of graphite) of approximately 12% corresponding to an under-moderated core. Both the diameter and the height of the reactor core are equal to 300 cm, while the thicknesses of radial and axial reflector are 50 and 20 cm, respectively. The geometry values selected in the study were only based on considering the neutron economy (the effective multiplication factor (k_{eff}). The density of the graphite for moderator and reflector was set as 1.86 g/cm^3.

The fuel salt composition included the carrier salt and heavy metals. FLiBe salt (2LiF–BeF_2) was selected as carrier salt by considering its excellent neutron economy and chemical and physical properties. As mentioned above, the proportion of heavy metals (HM proportion) in the fuel salt had a direct and significant impact on neutron spectrum and subsequently on neutronic characteristics such as breeding capability and temperature coefficient of reactivity. The reduction in the HM proportion may have entailed an increase in the melting point of the fuel salt [23]. Furthermore, a higher melting point indicated that a higher operation temperature was required and led to a challenge with respect to the heat and irradiation resistance of the structural materials. Conversely, a higher proportion of carrier salt may cause higher neutron capture. Therefore, the minimum HM proportion was set as 2 mole%. Moreover, the upper limit of the HM proportion was set as 12 mole% by considering the solubility of heavy metals in fluoride salt and the feasibility to control oxygen. The mean operating temperature of the reactor was 880 K. Additionally, the ^{235}U enrichment was under 20%, given the non-proliferation, while the ^{7}Li enrichments of 99.95 and 99.995% were analyzed for comparison purposes.

2.2 Calculation of temperature coefficient

The analysis of the temperature coefficient (in this case, FSTC) was based on the six-factor formula as follows:

$$k_{\mathrm{eff}} = \varepsilon p \eta f \Lambda = \varepsilon p \eta f P_{\mathrm{FNL}} P_{\mathrm{TNL}}, \qquad (1)$$

where ε denotes the fast fission factor, p denotes the resonance escape probability, η denotes the thermal reproduction factor, f denotes the thermal utilization factor, and Λ denotes the total non-leakage probability that corresponds to the product of the fast (P_{FNL}) and the thermal (P_{TNL}) non-leakage probability. Thus, five factors, i.e., ε, p, η, f, and Λ, were adopted to calculate FSTC.

The FSTC (α_{T}) is a measure of the variation in k_{eff} (Δk) with the temperature of fuel salt (ΔT) as follows:

$$\alpha_T = \frac{\Delta k}{\Delta T} = \frac{k_2 - k_1}{T_2 - T_1}. \qquad (2)$$

The change in the fuel salt temperature can lead to a variation in neutron spectrum, and subsequently an alteration of k_{eff}. Thus, each factor in the six-factor formula is related to the temperature and is used to clarify the FSTC. Therefore, the FSTC was separated into five components ($\alpha_{\mathrm{T}}(\varepsilon), \alpha_{\mathrm{T}}(p), \alpha_{\mathrm{T}}(\eta), \alpha_{\mathrm{T}}(f)$, and $\alpha_{\mathrm{T}}(\Lambda)$) by taking the derivative of Eq. (1) with respect to temperature as follows:

$$\begin{aligned}\alpha_{\mathrm{T}} &= C_1\alpha'_{\mathrm{T}}(\varepsilon) + C_2\alpha'_{\mathrm{T}}(p) + C_3\alpha'_{\mathrm{T}}(\eta) + C_4\alpha'_{\mathrm{T}}(f) + C_5\alpha'_{\mathrm{T}}(\Lambda) \\ &= \alpha_{\mathrm{T}}(\varepsilon) + \alpha_{\mathrm{T}}(p) + \alpha_{\mathrm{T}}(\eta) + \alpha_{\mathrm{T}}(f) + \alpha_{\mathrm{T}}(\Lambda),\end{aligned} \qquad (3)$$

where $C_1 = p\eta f\Lambda, C_2 = \varepsilon\eta f\Lambda, C_3 = \varepsilon p f\Lambda, C_4 = \varepsilon p\eta\Lambda$, $C_5 = \varepsilon p\eta f$. Each factor with the superscript of left-hand diagonal ($\alpha'_{\mathrm{T}}(\varepsilon), \alpha'_{\mathrm{T}}(p), \alpha'_{\mathrm{T}}(\eta), \alpha'_{\mathrm{T}}(f), \alpha'_{\mathrm{T}}(\Lambda)$) was estimated successively for two temperatures as follows:

$$\alpha'_{\mathrm{T}}(F) = \frac{\Delta F}{\Delta T} = \frac{F_2 - F_1}{T_2 - T_1} \qquad (4)$$

where F denote ε, p, η, f, or Λ.

2.3 Calculation tool

The MCNP5 code was adopted to perform all the neutronic calculations including the criticality and reactivity coefficients. Specifically, the concept of a universe was used to model the hierarchical geometry for MSR. The tally multiplier card, FMn, was employed to calculate the cross sections and subsequently to calculate the factors in the six-factor formula. In order to perform accurate calculations with the uranium-based fuels, an ACE (A Compact ENDF) format cross section library with continuous energy was chosen based on the ENDF/B-VII library. In order to improve the accuracy of the results, each criticality calculation was scheduled to skip 50 cycles and run a total of 200 cycles with nominally one million neutrons per cycle. The typical computing time of a criticality calculation was approximately 7 h with 16-point parallel computing.

3 Results and discussion

In order to understand the effects of fuel salt composition on FSTC, the interpretations of FSTC were initially discussed qualitatively via the six-factor formula (Sect. 3.1). Subsequently, the effects of the ^{235}U enrichment (Sect. 3.2), HM proportion (Sect. 3.3), and ^{7}Li enrichment (Sect. 3.4) on FSTC were investigated with quantitative parameters obtained from the simulation.

3.1 Six-factor contributions to FSTC

As mentioned previously, the FSTC is expressed as the sum of the five components via the six-factor formula (Eq. 3). Therefore, further research on the contributions (positive or negative) of the five components to FSTC is crucial for understanding how the fuel salt compositions affect FSTC for the variants of operation temperature. In order to quantitatively describe the neutron spectrum of a reactor, the energy of the average lethargy causing fission (EALF) was introduced, and it exhibited a higher value for a harder neutron spectrum and vice versa. Furthermore, the FSTC is a combination of the effect of the Doppler coefficient and density coefficient. Therefore, the contributions of the five components to the two effects were discussed in sequence as follows:

- The temperature coefficient $\alpha_T(\varepsilon)$ is significantly affected by the neutron spectrum. When the fuel salt temperature increases, the Doppler broadening leads to an increase in the resonance absorption and subsequently a decrease in the thermal neutron range, and thus, the neutron spectrum becomes harder corresponding to a higher EALF. Subsequently, the fast fission increases, and thus a positive $\alpha_T(\varepsilon)$ is shown for the Doppler coefficient. Conversely, the increases in fuel salt temperature lead to a reduction in the fuel salt density and a softer neutron spectrum corresponding to a smaller EALF due to the growing graphite-to-heavy metal ratio. This causes a decreased fast fission and leads to a negative $\alpha_T(\varepsilon)$ for the density coefficient.
- The temperature coefficient $\alpha_T(p)$ is also significantly dependent on the neutron spectrum. As discussed in the previous paragraph, for the Doppler coefficient, an increase in fuel salt temperature indicates that the neutron spectrum becomes harder and leads to a reduction of the resonance escape probability, and subsequently a negative $\alpha_T(p)$ is shown. Conversely, for the density coefficient, the sign of $\alpha_T(p)$ is positive.
- The temperature coefficient $\alpha_T(\eta)$ is mainly related to the fission reaction and the capture reaction of heavy metals. With respect to the uranium-based fuel, η is expressed as follows:

$$\eta = \frac{v_5 \Sigma_{f,th,5} + v_8 \Sigma_{f,th,8}}{\Sigma_{a,th,5} + \Sigma_{a,th,8}} \tag{5}$$

where v denotes the average number of neutrons released per fission, $\Sigma_{f,th}$ denotes the macroscopic thermal fission cross section, $\Sigma_{a,th}$ denotes the macroscopic thermal absorption cross section, and the subscripts 5 and 8 denote ^{235}U and ^{238}U, respectively. With the increases in fuel salt temperature, the Doppler broadening effect makes the neutron spectrum harder and weakens the thermal fission cross section and the absorption cross section. The variation in the thermal fission cross section is typically faster than that of the thermal absorption cross section mainly due to the fertile nuclide (^{238}U for the uranium-based fuel, see Fig. 2). Thus, a reduction in η is introduced and a negative $\alpha_T(\eta)$ is displayed for the Doppler coefficient. Conversely, the increases in fuel salt temperature reduce the fuel salt density and increase the C/HM (the atom ratio of graphite and heavy metals). Subsequently, the Maxwell's spectrum becomes wider and its peak increases, and thus the neutron spectrum becomes softer. In this case, the fission cross sections increase faster than the absorption cross sections (Fig. 2). Therefore, a higher η is introduced and a positive $\alpha_T(\eta)$ is exhibited for the density coefficient.
- The temperature coefficient $\alpha_T(f)$ depends on the effect of the atomic density of fuel salt and graphite over that of neutron spectrum. With respect to a graphite-moderated MSR, f was calculated as follows:

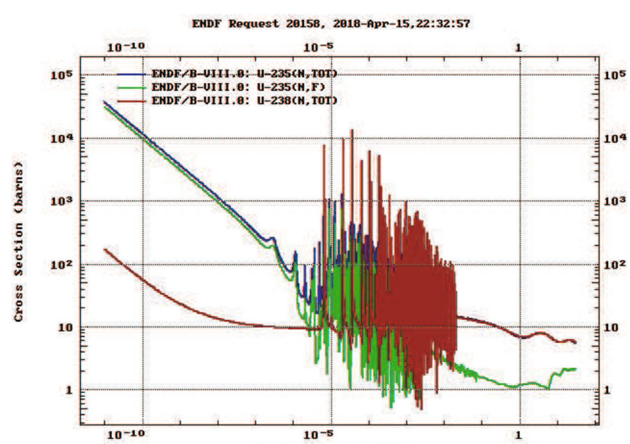

Fig. 2 (Color online) The cross sections of ^{235}U and ^{238}U

$$f = \frac{\sum_{HM} \Sigma_{a,th}}{\sum_{HM,FLiBe,C} \Sigma_{a,th}} \quad (6)$$

where the numerator denotes the thermal absorption of heavy metals (HM), while the denominator denotes the thermal absorption in total including the heavy metals, FLiBe salt, and graphite (labeled C). When the fuel salt temperature increases, the Doppler coefficient makes the neutron spectrum harder and weakens the thermal absorption for all elements, while the density coefficient leads to an opposite tendency. The relative change in the thermal absorption of heavy metals is comparable to that of FLiBe, and thus the variation in f is mainly dependent on the relative variation in graphite and heavy metals. The calculations show that the Doppler coefficient causes the thermal absorption of heavy metals to decrease faster than graphite while the density coefficient causes the thermal absorption of graphite to increase faster than heavy metals. Subsequently, a reduction in f is introduced and displays a negative $\alpha_T(f)$ either for the Doppler coefficient or the density coefficient.

- The temperature coefficient $\alpha_T(\Lambda)$ is closely related to neutron diffusion. With respect to the Doppler coefficient, when the fuel salt temperature increases, the widening neutron spectrum enhances the resonance absorption. Hence, the slowing-down time of fast neutrons increases and leads to a decrease in the fast non-leakage probability (P_{FNL}). Furthermore, for the Density coefficient, the reduction in the fuel salt density weakens the collision probability between thermal neutrons and heavy metals, and thus, the thermal neutron diffusion length increases and decreases the thermal non-leakage probability (P_{TNL}). Therefore, the total non-leakage probability (Λ) decreases and a negative $\alpha_T(\Lambda)$ is shown for both the Doppler coefficient and the density coefficient.
  Furthermore, the main contribution to Λ corresponds to P_{TNL} due to the significantly longer diffusion time relative to the slowing-down time. An increase in the softness of the neutron spectrum increases the significance of the variation in k_{eff} with a small change in Λ, and thus a stronger $\alpha_T(\Lambda)$ is introduced. In an under-moderated core of MSR, when the ^{235}U enrichment and/or HM changes, the neutron spectrum is still relatively hard, and subsequently, the change in $\alpha_T(\Lambda)$ is insignificant when compared with that of $\alpha_T(p)$ and $\alpha_T(\varepsilon)$ and is not shown in Sects. 3.2 and 3.3. However, the neutron spectrum tends to be softer with the variation in ^{7}Li enrichment, and the contribution of $\alpha_T(\Lambda)$ to FSTC should be increasingly focused and is discussed in Sect. 3.4.

Table 1 Six-factor contributions to the Doppler and density coefficient

	Doppler	Density
$\alpha_T(\varepsilon)$	+	−
$\alpha_T(p)$	−	+
$\alpha_T(\eta)$	−	+
$\alpha_T(f)$	−	−
$\alpha_T(\Lambda)$	−	−

Based on the above discussions, Table 1 shows the sign of the five components. Here, "+" and "−" denote a positive and negative temperature coefficient, respectively. With respect to the Doppler coefficient, the sign of $\alpha_T(\varepsilon)$ is positive, while the other four are negative. With respect to the density coefficient, the sign of $\alpha_T(p)$ and $\alpha_T(\eta)$ are positive, while the other three are negative.

3.2 Effect of ^{235}U enrichment on FSTC

With respect to the uranium-based fuel, the ^{235}U enrichment impacts the neutron spectrum and subsequently the microcosmic and/or macroscopic cross section of heavy metals. Figure 3 shows the trends of EALF with ^{235}U enrichment for different HM proportions. As shown in the figure, an increase in the HM proportion and/or an increase in ^{235}U enrichment increases the EALF corresponding to a harder spectrum. Furthermore, the value of EALF is more sensitive to the ^{235}U enrichment for a higher HM proportion due to its harder spectrum.

The variation in the FSTC with the ^{235}U enrichment for different HM proportion is shown in Fig. 4. The FSTC is always negative for all ^{235}U enrichments and HM proportions. With respect to a fixed HM proportion, when the ^{235}U enrichment increases, the magnitude of FSTC initially increases and subsequently decreases, and the turning point corresponds to a higher ^{235}U enrichment for a lower HM proportion. It should be noted that the difference in the

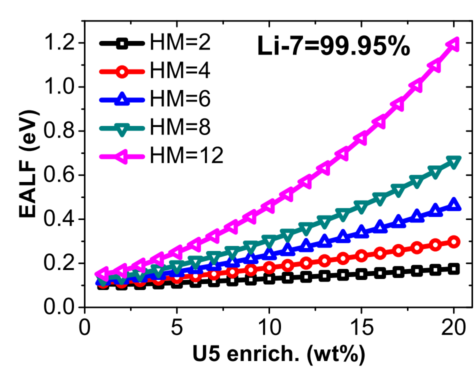

Fig. 3 (Color online) EALF as a function of ^{235}U enrichment for different HM proportions

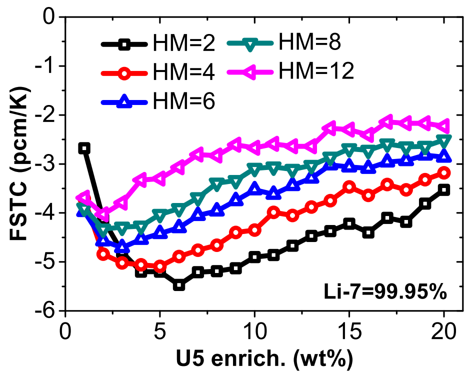

Fig. 4 (Color online) FSTC as a function of ^{235}U enrichment for different HM proportions

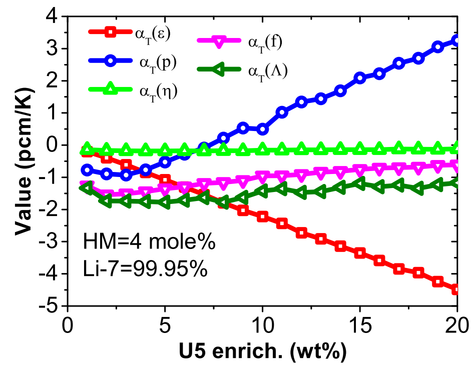

Fig. 6 (Color online) Variations in $\alpha_T(\varepsilon)$ and $\alpha_T(p)$ for FSTC with ^{235}U enrichment

FSTC between any two HM proportions is almost independent of the ^{235}U enrichment after the turning point.

In order to further understand the above phenomena, Fig. 5 shows the variations in FSTC and its two separate effects with ^{235}U enrichment for HM = 4 mole% as an example. First, the Doppler coefficient is always negative for any ^{235}U enrichment. When the ^{235}U enrichment increases, the magnitude of the Doppler coefficient initially increases and subsequently becomes almost saturated due to the gradually hardening spectrum that is more favorable to the resonances of ^{238}U (main resonances located between 6.7 eV and 20 keV while those of ^{235}U are between 4.8 eV and 2.2 keV). Second, when the ^{235}U enrichment increases, the density coefficient changes from negative to positive. In an under-moderated core, a decrease in fuel salt density allows for increased moderation and thus softens the neutron spectrum that leads to a higher fission rate. Subsequently, a positive density coefficient is typically observed. Furthermore, a negative density coefficient at low enrichment possibly implies that the core is near over-moderation. In this case, a decrease in the fuel salt density can lead to increased parasitic absorptions in the graphite that decrease the fission rate, thereby introducing a negative coefficient. Thus, a combination of the above two effects initially strengthens the FSTC and subsequently weakens it when the ^{235}U enrichment increases.

Based on Eq. (4), the variations in the five components for FSTC with the ^{235}U enrichment are shown in Fig. 6. The results indicate that the sign of $\alpha_T(\varepsilon)$ is negative, and its magnitude increases when the ^{235}U enrichment increases. Furthermore, the sign of $\alpha_T(p)$ changes from less negative to more positive. Additionally, the signs of $\alpha_T(f)$ and $\alpha_T(\Lambda)$ are negative and they both weaken with increase in the ^{235}U enrichment. Although their variations with respect to the ^{235}U enrichment are significantly less than those of $\alpha_T(\varepsilon)$ and $\alpha_T(p)$, their magnitudes cannot be neglected. Moreover, the magnitude of $\alpha_T(\eta)$ is almost zero for all the ^{235}U enrichment. Therefore, as a whole, the magnitude of FSTC (black square in Fig. 5) initially mainly increases due to $\alpha_T(\varepsilon)$ and subsequently mainly decreases due to $\alpha_T(p)$.

Furthermore, the values of $\alpha_T(\varepsilon)$ and $\alpha_T(p)$ for FSTC are separated into the Doppler and density contributions as

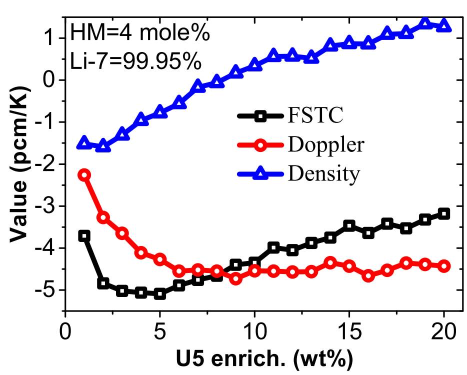

Fig. 5 (Color online) FSTC, Doppler and Density coefficient as a function of ^{235}U enrichment for HM = 4 mole%

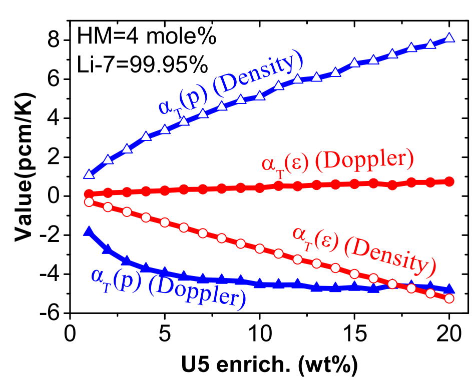

Fig. 7 (Color online) Variations in $\alpha_T(\varepsilon)$ and $\alpha_T(p)$ for Doppler and Density with ^{235}U enrichment

shown in Fig. 7. Thus, when the ^{235}U enrichment increases, the absolute value of $\alpha_T(\varepsilon)$ and $\alpha_T(p)$ increases for both the Doppler coefficient and the density coefficient due to the hardening neutron spectrum. As interpreted in Sect. 3.1 (Table 1), the sign of $\alpha_T(\varepsilon)$ for the Doppler coefficient and that of $\alpha_T(p)$ for the density coefficient are positive, while that of $\alpha_T(\varepsilon)$ for the density coefficient and that of $\alpha_T(p)$ for the Doppler coefficient are negative. In conjunction with Figs. 6 and 7, the magnitude and the sign of $\alpha_T(\varepsilon)$ and $\alpha_T(p)$ for FSTC that varies with the ^{235}U enrichment is primarily due to the density coefficient.

In summary, the effect of the ^{235}U enrichment on FSTC is mainly dependent on the density coefficient especially for its $\alpha_T(\varepsilon)$ and $\alpha_T(p)$. In order to obtain an sufficiently negative FSTC, a lower ^{235}U enrichment is recommended to suppress the positive $\alpha_T(p)$ for the density coefficient.

3.3 Effect of HM proportion on FSTC

With respect to a liquid-fueled MSR, the proportion of heavy metals (HM proportion) in the fuel salt phase diagram is closely related with the neutron spectrum. A change in the HM proportion, accordingly, shifts the neutron spectrum, and subsequently, a high variation in the microscopic cross sections of heavy metals is introduced that alters the FSTC. In order to understand the effects of the HM proportion on FSTC, the ^{235}U enrichment and the ^{7}Li enrichment are set as constants with values of 19.75 and 99.95%, respectively.

The variations in FSTC and its two separate effects with the HM proportion are shown in Fig. 8. When the HM proportion increases, the Doppler coefficient strengthens and always remains negative, while the density coefficient varies from less negative (nearly zero) to more positive. With respect to the aforementioned two effects, the FSTC is mainly attributed to the effect of the density coefficient, and its value is negative and weakens with increases in the HM proportion.

Figure 9 shows the variations in $\alpha_T(\varepsilon)$ and $\alpha_T(p)$ for FSTC, Doppler coefficient, and the density coefficient with increases in HM proportion with a constant ^{235}U enrichment. As shown in the left figure, the signs of $\alpha_T(\varepsilon)$ and $\alpha_T(p)$ are opposite, and their magnitudes increase when the HM proportion increases. The other three factors ($\alpha_T(\eta), \alpha_T(f)$, and $\alpha_T(\Lambda)$) for FSTC are not shown due to their significantly lower sensitivity to the HM proportions. Furthermore, as shown in the right figure, the signs of $\alpha_T(\varepsilon)$ and $\alpha_T(p)$ for the two separate effects are consistent with those in Table 1. In a manner similar to Fig. 7, the magnitudes of $\alpha_T(\varepsilon)$ and $\alpha_T(p)$ for both the Doppler coefficient and the density coefficient increase when the HM proportion increases because the neutron spectrum becomes harder. Given the above considerations, $\alpha_T(\varepsilon)$ and $\alpha_T(p)$ for FSTC are mainly affected by the density coefficient.

In summary, recommendations include lowering HM proportion to suppress the possible density coefficient and to achieve an sufficiently negative FSTC. Additionally, it is important to note that lowering the HM proportion is conducive to oxygen control although it results in a higher melting point for the fuel salt mixture.

3.4 Effect of ^{7}Li enrichment on FSTC

The carrier salt FLiBe exhibits good compatibility with structure material, including nuclear grade graphite and hastelloy. This is verified by the molten salt reactor experiment (MSRE) [24]. Enriched ^{7}Li is recommended given its smaller thermal neutron absorption cross section that is important in improving the neutron economy and suppressing the undesired tritium production [25]. Furthermore, the enrichment of ^{7}Li is highly correlated with neutronic properties such as the neutron spectrum, the critical ^{235}U enrichment, and FSTC. The ^{235}U enrichment

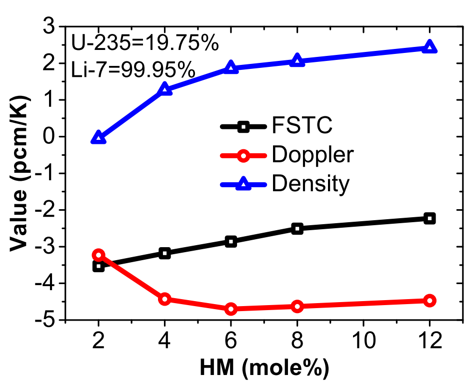

Fig. 8 (Color online) FSTC, Doppler, and Density coefficient as a function of the HM proportion with ^{235}U enrichment of 19.75% and ^{7}Li enrichment of 99.95%

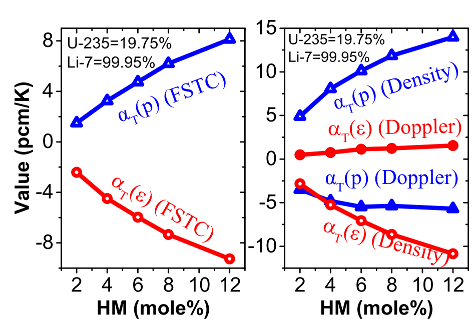

Fig. 9 (Color online) Variations in $\alpha_T(\varepsilon)$ and $\alpha_T(p)$ with the HM proportion for FSTC (left) and its two separate coefficients (right) with fixed ^{235}U enrichment

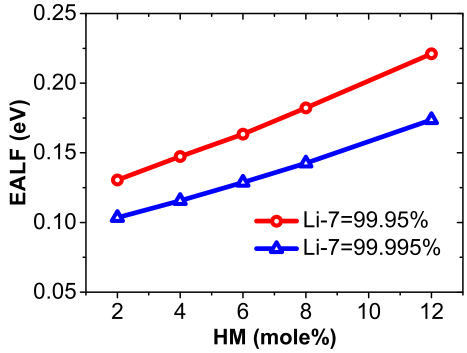

Fig. 10 (Color online) Variation in EALF with the HM proportion for two ^{7}Li enrichments

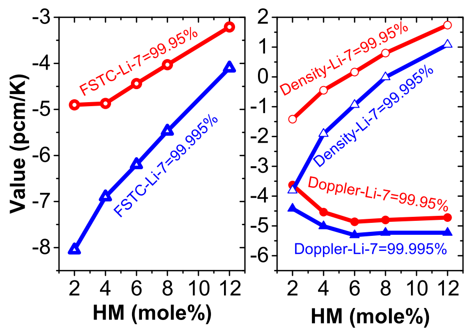

Fig. 11 (Color online) Variation in FSTC (left) and its two separate effects (right) with the HM proportion for different ^{7}Li enrichment

used in this section is less than 10 wt% to achieve criticality for all the HM proportions.

The neutron spectra of two types of ^{7}Li enrichment for different HM proportion are quantified as EALF and shown in Fig. 10. The results indicate that a higher ^{7}Li enrichment exhibits a smaller EALF corresponding to a softer neutron spectrum due to reduced thermal absorption from ^{6}Li.

Figure 11 shows the effects of ^{7}Li enrichment on FSTC (left) and its two separate effects (right) with the HM proportion. As shown in the left figure, a higher ^{7}Li enrichment corresponds to a softer spectrum, and thus even a small change in the ^{7}Li enrichment can cause a significant variation in k_{eff}, and subsequently, a more negative FSTC. Furthermore, an increase in the ^{7}Li enrichment makes the variation of FSTC between different HM proportions increasingly significant. As shown in the right figure, the results indicate that a higher ^{7}Li enrichment leads to a more negative Doppler coefficient for all HM proportions and more negative and less positive density coefficients for the lower HM proportions and higher HM proportions, respectively. Furthermore, a decrease in the HM proportion increases the proportion of FLiBe, and this increases the difference between FSTC for the two ^{7}Li enrichments, which is mainly due to the density coefficient.

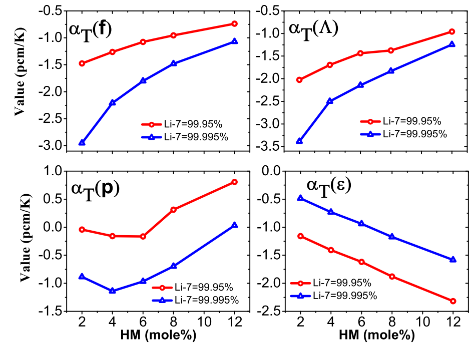

Fig. 12 (Color online) Variations in $\alpha_{\mathrm{T}}(f), \alpha_{\mathrm{T}}(\Lambda), \alpha_{\mathrm{T}}(p)$ and $\alpha_{\mathrm{T}}(\varepsilon)$ with the HM proportion for different ^{7}Li enrichment values

In order to further understand the effect of the ^{7}Li enrichment on FSTC, Fig. 12 shows the variations in $\alpha_{\mathrm{T}}(f), \alpha_{\mathrm{T}}(\Lambda), \alpha_{\mathrm{T}}(p)$ and $\alpha_{\mathrm{T}}(\varepsilon)$ along with the HM proportion for the two ^{7}Li enrichments. The results indicate that for all the HM proportions, a higher ^{7}Li enrichment leads to a more negative $\alpha_{\mathrm{T}}(f), \alpha_{\mathrm{T}}(\Lambda)$ and $\alpha_{\mathrm{T}}(p)$ especially for the former two cases due to their more sensitive dependence on the shift of neutron spectrum. In parallel, a lower ^{7}Li enrichment leads to a more negative $\alpha_{\mathrm{T}}(\varepsilon)$ benefited from a harder spectrum. It should be noted that although the variation in $\alpha_{\mathrm{T}}(\eta)$ along with the HM proportion exhibits a similar trend as $\alpha_{\mathrm{T}}(f)$ for two ^{7}Li enrichments, its value is almost excessively low to be considered. In summary, enhancements in ^{7}Li enrichment are recommended to gain a more negative FSTC.

4 Conclusion

A sufficiently negative fuel salt temperature coefficient (FSTC) is crucial to compensate for a possible positive moderator temperature coefficient (MTC) in a graphite-moderated MSR with liquid fuel. Fuel salt compositions strongly affect the FSTC in terms of the ^{235}U enrichment, heavy metal proportion in the salt phase (HM), and the ^{7}Li enrichment, and this is investigated using a six-factor formula for an under-moderated core.

The FSTC is a combination of the Doppler coefficient and the density coefficient, both of which are closely related to the neutron spectrum. In order to further understand the effects of FSTC, the temperature coefficients of the five factors based on the six-factor formula was introduced and includes $\alpha_{\mathrm{T}}(\varepsilon), \alpha_{\mathrm{T}}(p), \alpha_{\mathrm{T}}(\eta), \alpha_{\mathrm{T}}(f)$, and $\alpha_{\mathrm{T}}(\Lambda)$. With respect to the Doppler coefficient, when the fuel salt temperature increases, the neutron spectrum becomes harder due to the enhancing resonance absorption and the rising EALF. Thus, the temperature coefficient of ε ($\alpha_{\mathrm{T}}(\varepsilon)$)

is positive, while the other four are negative. With respect to the density coefficient, with increase in the fuel salt temperature, the neutron spectrum becomes softer due to the reducing fuel salt density and the declined EALF. Therefore, the temperature coefficients of p ($\alpha_T(p)$) and η ($\alpha_T(\eta)$) are positive while the other three are negative.

The FSTC is affected by the ^{235}U enrichment and the HM proportion via the neutron spectrum and is more significantly influenced by the density coefficients. From the viewpoint of the six-factor formula, the above effects are reflected in $\alpha_T(p)$ and $\alpha_T(\varepsilon)$ if the neutron spectrum is relatively hard. With respect to a fixed HM proportion, the FSTC is always negative and its magnitude initially increases due to the increased negative Doppler coefficient (mainly $\alpha_T(p)$) and subsequently decreases due to the weakening negative or the increases in positive density coefficient (the synergistic effects of $\alpha_T(p)$ and $\alpha_T(\varepsilon)$) when the ^{235}U enrichment increases. If the ^{235}U enrichment exceeds a certain value, the FSTC strengthens with increases in the HM proportion. Thus, recommendations include lowering the HM proportion and/or lowering the ^{235}U enrichment to obtain a more negative FSTC. Moreover, the effects of the ^{7}Li enrichment on FSTC are achieved by the neutron absorption and also mainly determined by $\alpha_T(f)$ and $\alpha_T(\Lambda)$ if the neutron spectrum is relatively soft. The enhancement of the ^{7}Li enrichment results in a reduction in the critical ^{235}U enrichment and leads to a more negative FSTC.

The analyses provide insight into the influence of the fuel salt compositions on the FSTC from the aspect of the six-factor formula for an under-moderated MSR. It may be concluded that a reduction in the ^{235}U enrichment and/or the HM proportion and an improvement in the ^{7}Li enrichment are necessary to gain a more negative FSTC by suppressing the possible positive density coefficient. The density coefficient is extremely significant and its analysis must always include a discussion on the moderation ratio values of the reactor core. Hence, further studies are required to confirm the applicability of the above results for an over-moderated MSR. Furthermore, the effects of fuel salt compositions with different values of burn-up, various types of heavy metals, and/or different operation temperatures on FSTC should be evaluated on a core level. This will make it possible to implement a more feasible fuel salt composition for a sufficiently negative FSTC.

References

1. D. LeBlanc, Molten salt reactors: a new beginning for an old idea. Nucl. Eng. Des. **240**, 1644–1656 (2010). https://doi.org/10.1016/j.nucengdes.2009.12.033
2. J. Serp, M. Allibert, O. Beneš et al., The molten salt reactor (MSR) in generation IV: overview and perspectives. Prog. Nucl. Energy **77**, 308–319 (2014). https://doi.org/10.1016/j.pnucene.2014.02.014
3. J.E. Kelly, Generation IV International Forum: A decade of progress through international cooperation. Prog. Nucl. Energy **77**, 240–246 (2014). https://doi.org/10.1016/j.pnucene.2014.02.010
4. R.C. Robertson, Conceptual design study of a single-fluid molten-salt breeder reactor. Oak Ridge National Lab. ORNL–4541 (1971). https://doi.org/10.2172/4030941
5. E. Merle-Lucotte, D. Heuer, M. Allibert et al., Optimization and simplification of the concept of non-moderated thorium molten salt reactor, in *International Conference on the Physics of Reactors-PHYSOR 2008*, Sept. 2008. in2p3-00326466 (Interlaken, Switzerland, 2008), pp. 14–19
6. R.O. Scarlat, P.F. Peterson, The current status of fluoride salt cooled high temperature reactor (FHR) technology and its overlap with HIF target chamber concepts. Nucl. Instrum. Methods A **733**, 57–64 (2014). https://doi.org/10.1016/j.nima.2013.05.094
7. C. Forsberg, The advanced high-temperature reactor: high-temperature fuel, liquid salt coolant, liquid-metal-reactor plant. Prog. Nucl. Energy **47**, 32–43 (2005). https://doi.org/10.1016/j.pnucene.2005.05.002
8. G. Locatelli, M. Mancini, N. Todeschini, Generation IV nuclear reactors: current status and future prospects. Energy Policy **61**, 1503–1520 (2013). https://doi.org/10.1016/j.enpol.2013.06.101
9. T. Kamei, S. Hakami, Evaluation of implementation of thorium fuel cycle with LWR and MSR. Prog. Nucl. Energy **53**, 820–824 (2011). https://doi.org/10.1016/j.pnucene.2011.05.032
10. E. Merle-Lucotte, D. Heuer, M. Allibert, et al., Optimized transition from the reactors of second and third generations to the Thorium Molten Salt Reactor, in *ICAPP 2007: International Congress on Advances in Nuclear Power Plants*, May 2007. in2p3-00135149 (American Nuclear Society, Nice, France, 2007), p. 7186
11. A. Nuttin, D. Heuer, A. Billebaud et al., Potential of thorium molten salt reactors detailed calculations and concept evolution with a view to large scale energy production. Prog. Nucl. Energy **46**, 77–99 (2005). https://doi.org/10.1016/j.pnucene.2004.11.001
12. J. Žáková, A. Talamo, Analysis of the reactivity coefficients of the advanced high-temperature reactor for plutonium and uranium fuels. Ann. Nucl. Energy **35**, 904–916 (2008). https://doi.org/10.1016/j.anucene.2007.09.003
13. L. Mathieu, D. Heuer, R. Brissot et al., The thorium molten salt reactor: moving on from the MSBR. Prog. Nucl. Energy **48**, 664–679 (2006). https://doi.org/10.1016/j.pnucene.2006.07.005
14. J. Křepel, U. Rohde, U. Grundmann et al., Dynamics of molten salt reactors. Nucl. Technol. **164**, 34–44 (2008). https://doi.org/10.13182/NT08-A4006
15. L. Mathieu, D. Heuer, A. Nuttin et al., Thorium molten salt reactor: from high breeding to simplified reprocessing, in *GLOBAL 2003-Nuclear Science and Technology: Meeting the Global Industrial and R&D Challenges of the 21st Century*, Nov. 2003. in2p3-00020302 (American Nuclear Society, New Orleans, USA, 2003), pp. 1863–1872
16. S.C. Tadepalli, A. Gupta, K. Umasankari, Neutronic analysis of msre and its study for validation of arch code. Nucl. Eng. Des. **320**, 1–8 (2017). https://doi.org/10.1016/j.nucengdes.2017.05.005
17. P.N. Haubenreich, J.R. Engel, B.E. Prince et al., MSRE Design and Operations Report. Part III. Nuclear analysis. Oak Ridge National Lab. ORNL-TM-730 (1964)
18. J. Křepel, B. Hombourger, C. Fiorina et al., Fuel cycle advantages and dynamics features of liquid fueled MSR. Ann. Nucl. Energy **64**, 380–397 (2014). https://doi.org/10.1016/j.anucene.2013.08.007

19. S.Y. Si, Q.C. Chen, H. Bei et al. New exploration on TMSR: The lattice optimization, in *2014 22nd International Conference on Nuclear Engineering*. V003T05A010 (American Society of Mechanical Engineers, 2014). https://doi.org/10.1115/ICONE22-30220
20. E.E. Bende, Temperature reactivity effects in pebbles of a high-temperature reactor fueled with reactor-grade plutonium. Nucl. Technol. **131**, 279–296 (2000). https://doi.org/10.13182/NT00-A3117
21. C.Y. Li, R.J. Sheu, J.J. Peir et al., Neutronic analysis of the HTTR core fueled with plutonium and minor actinides, in *2013 21st International Conference on Nuclear Engineering*. V002T05A056 (American Society of Mechanical Engineers, 2013). https://doi.org/10.1115/ICONE21-16507
22. N.Z. Zainuddin, G.T. Parks, E. Shwageraus, The factors affecting MTC of thorium–plutonium–fuelled PWRs. Ann. Nucl. Energy **98**, 132–143 (2016). https://doi.org/10.1016/j.anucene.2016.07.034
23. E. Merle-Lucotte, L. Mathieu, D. Heuer et al., Influence of the processing and salt composition on the thorium molten salt reactor. Nucl. Technol. **163**, 358–365 (2008). https://doi.org/10.13182/NT08-A3994
24. R.C. Robertson, MSRE Design and Operations Report. Part I. Description of Reactor Design. Oak Ridge National Lab. ORNL-TM-728 (1965). https://doi.org/10.2172/4654707
25. J.R. Keiser, J.H. DeVan, D.L. Manning, Corrosion resistance of type 316 stainless steel to Li_2BeF_4. Oak Ridge National Lab. ORNL/TM–5782 (1977). https://doi.org/10.2172/7110792